The EMBO Journal vol.13 no.9 pp.2218-2226, 1994

Efficient aminoacylation of resected RNA helices by class II aspartyl-tRNA synthetase dependent on a single nucleotide

Magali Frugier, Catherine Florentz and Richard Giegé[1]

Unité Structure des Macromolécules Biologiques et Mécanismes de Reconnaissance, Institut de Biologie Moléculaire et Cellulaire du Centre National de la Recherche Scientifique, 15 rue René Descartes, F-67084 Strasbourg Cedex, France
[1]Corresponding author

Communicated by M.Sprinzl

We show here that small RNA helices which recapitulate part or all of the acceptor stem of yeast aspartate tRNA are efficiently aminoacylated by cognate class II aspartyl-tRNA synthetase. Aminoacylation is strongly dependent on the presence of the single-stranded G73 'discriminator' identity nucleotide and is essentially insensitive to the sequence of the helical region. Substrates which contain as few as 3 bp fused to G73CCA$_{OH}$ are aspartylated. Their charging is insensitive to the sequence of the loop closing the short helical domains. Aminoacylation of the aspartate mini-helix is not stimulated by a hairpin helix mimicking the anticodon domain and containing the three major anticodon identity nucleotides. A thermodynamic analysis demonstrates that enzyme interactions with G73 in the resected RNA substrates and in the whole tRNA are the same. Thus, if the resected RNA molecules resemble in some way the earliest substrates for aminoacylation with aspartate, then the contemporary tRNA^{Asp} has quantitatively retained the influence of the major signal for aminoacylation in these substrates.
Key words: aminoacylation/aspartyl-tRNA synthetase/evolution/RNA mini-helices/tRNA identity

Introduction

According to the present view, specific tRNA aminoacylation is ensured when identity elements on the nucleic acid are presented towards aminoacyl-tRNA synthetases (aaRSs) to activate their catalytic center by mechanisms still not well understood but triggered by the identity nucleotides contacting sensitive identity amino acids on the protein (reviewed by Giegé *et al.*, 1993). This implies that RNA structures deviating from canonical tRNAs may be aminoacylated, provided identity elements can fulfil their recognition role. This is the case in viral tRNA-like structures, which represent macrosubstrates of synthetases (reviewed by Florentz and Giegé, 1994), but also in minimalist RNA structures. Indeed, because of the symmetric architecture of tRNA, with well separated amino acid-accepting and anticodon-containing domains, it becomes possible to dissect the molecule into its two individual components. Taking advantage of this fact, it was shown in the case of alanine systems, where the G3-U70 identity base pair is located near to the CCA$_{OH}$-end of the tRNA, that mini-helices mimicking the accepting branch of alanine-specific tRNAs can be specifically aminoacylated (Francklyn and Schimmel, 1989). It was also shown for systems in which identity elements are distributed in both domains of the tRNA, that individual anticodon hairpin loops can interact specifically with synthetases (Meinnel *et al.*, 1991) and can even improve aminoacylation of accepting mini-helices (Frugier *et al.*, 1992; Nureki *et al.*, 1993).

After the first studies on alanine-specific mini-helices, chargeable RNA mini-substrates of synthetases have been found in six other systems (reviewed by Musier-Forsyth and Schimmel, 1993; Schimmel *et al.*, 1993). They include 12 bp mini-helices specific for glycine (Francklyn *et al.*, 1992), histidine (Francklyn and Schimmel, 1990), isoleucine (Nureki *et al.*, 1993), methionine (Martinis and Schimmel, 1992a,b), serine (Sampson and Saks, 1993) and valine (Frugier *et al.*, 1992). Generalizing the idea that RNAs can become substrates of synthetases, provided identity elements are properly located in their structure, led to the design of alternative minimalist structures; that is of a mini-helix containing a pseudoknot which is charged by yeast HisRS (Rudinger *et al.*, 1992a), of micro-helices of reduced size closed by T-loops or tetraloops (Francklyn and Schimmel, 1989, 1990; Francklyn *et al.*, 1992; Martinis and Schimmel, 1992a,b), of RNA-RNA or RNA-DNA duplexes (Musier-Forsyth and Schimmel, 1992, 1993), and even of single-stranded RNAs (Khvorova *et al.*, 1992).

When comparing mini-helix aminoacylation in the different systems studied to date, it appears that efficient charging occurs when major identity elements are mainly (or exclusively) included within the mini-helix itself (e.g. in alanine, glycine and histidine systems). Significant levels of mini-helix charging also occur in the serine system, in which the major contribution for identity originates from the tRNA extra-loop/stem structure (Sampson and Saks, 1993). In contrast, when identity elements are distributed over the whole tRNA structure and include anticodon positions (e.g. in methionine, isoleucine and valine systems), mini-helix aminoacylation is generally less efficient. These functional differences may be correlated with the ranking of synthetases into two classes (Cusack *et al.*, 1990; Eriani *et al.*, 1990). Class I synthetases (IleRS, MetRS, ValRS), that always require tRNA determinants in the anticodon, seem to charge RNA mini-helices less efficiently than class II enzymes (AlaRS, GlyRS, HisRS, SerRS) for which anticodon is not an absolute requirement for activity.

Here we address the question of the chargeability by class II yeast AspRS of RNA helices resected from yeast tRNA^{Asp} and other non-cognate tRNAs. Experiments show that mini-helices recapitulating the acceptor branch of tRNA can be charged at high levels, provided they contain a G residue at discriminator position 73. Chargeability is retained for simplified versions of the canonical tRNA^{Asp} mini-helix. This demonstrates that aspartate mini-helices containing only

identity determinant G73 can function independently without participation of the four determinants (base pair G10-U25 and anticodon residues G34, U35 and C36; Pütz *et al.*, 1991) present in the missing domain of the tRNA. These data will be rationalized taking into account the specific structural and functional characteristics of the AspRS–tRNA^{Asp} complex (Ruff *et al.*, 1991; Cavarelli *et al.*, 1993; Pütz *et al.*, 1993). Mechanistic and evolutionary implications are discussed.

Results

Design of minimalist substrates for yeast AspRS

Figure 1 displays the secondary structure of the whole yeast tRNA^{Asp} and of the 11 RNA molecules that were designed and prepared by *in vitro* transcription as minimalist substrates of yeast AspRS. Seven RNAs (molecules 2–8) are directly derived from the structure of the amino acid-accepting branch of yeast tRNA^{Asp}. Molecules 3–5 are variants at the discriminator site 73. Molecule 6 is a micro-helix built with the 7 bp stem corresponding to the amino acid-accepting stem of the tRNA closed by the tRNA^{Asp} T-loop. Molecules 7 and 8 are shortened micro-helices closed by a tetraloop 5′-UUCG-3′ of the UUNG-type. This tetraloop is of unusual stability (Cheong *et al.*, 1990) and was chosen as the T-loop mimic to increase the stability of the short helical stems of molecules 7 and 8. (For convenience these RNA mini-substrates will be named '*x* bp tetraloops' in this paper). Notice that the 3 and 4 bp tetraloops are present in the helical part of the sequence of yeast tRNA^{Asp}; thus the loop closes a 5′-G-C-3′ pair in molecule 7 and an inverted 5′-C-G-3′ pair in molecule 8. Molecule 12 is a hairpin helix corresponding to the anticodon stem of tRNA^{Asp}.

Mini-helices 9–11 correspond to sequences of non-cognate tRNAs for yeast AspRS, but all contain a G residue at discriminator position 73. *Escherichia coli* mini-helix^{Asp} is a domain of a tRNA efficiently charged by yeast AspRS (Pütz *et al.*, 1991). This is not the case in mini-helix^{Arg} and mini-helix^{Gln}, the mimics of the accepting branches of yeast tRNA^{Arg} and *E.coli* tRNA^{Gln} which are only poorly mischarged by yeast AspRS (Ebel *et al.*, 1973). Notice that the sequences of the T-loops of these mini-helices all differ from that of yeast tRNA^{Asp}.

Aspartylation of wild-type mini-helix^{Asp}

Mini-helix^{Asp} corresponds to an RNA hairpin mimicking exactly the acceptor stem (7 bp plus four single-stranded nucleotides) and T-stem (5 bp) and loop (7 nt long) of yeast tRNA^{Asp} (Figure 1). This structure containing only one identity nucleotide, namely residue G73 at the discriminator position, has been synthesized by *in vitro* transcription of single-stranded templates. It is significantly charged by yeast AspRS. As seen in Figure 2A, aminoacylation plateaus

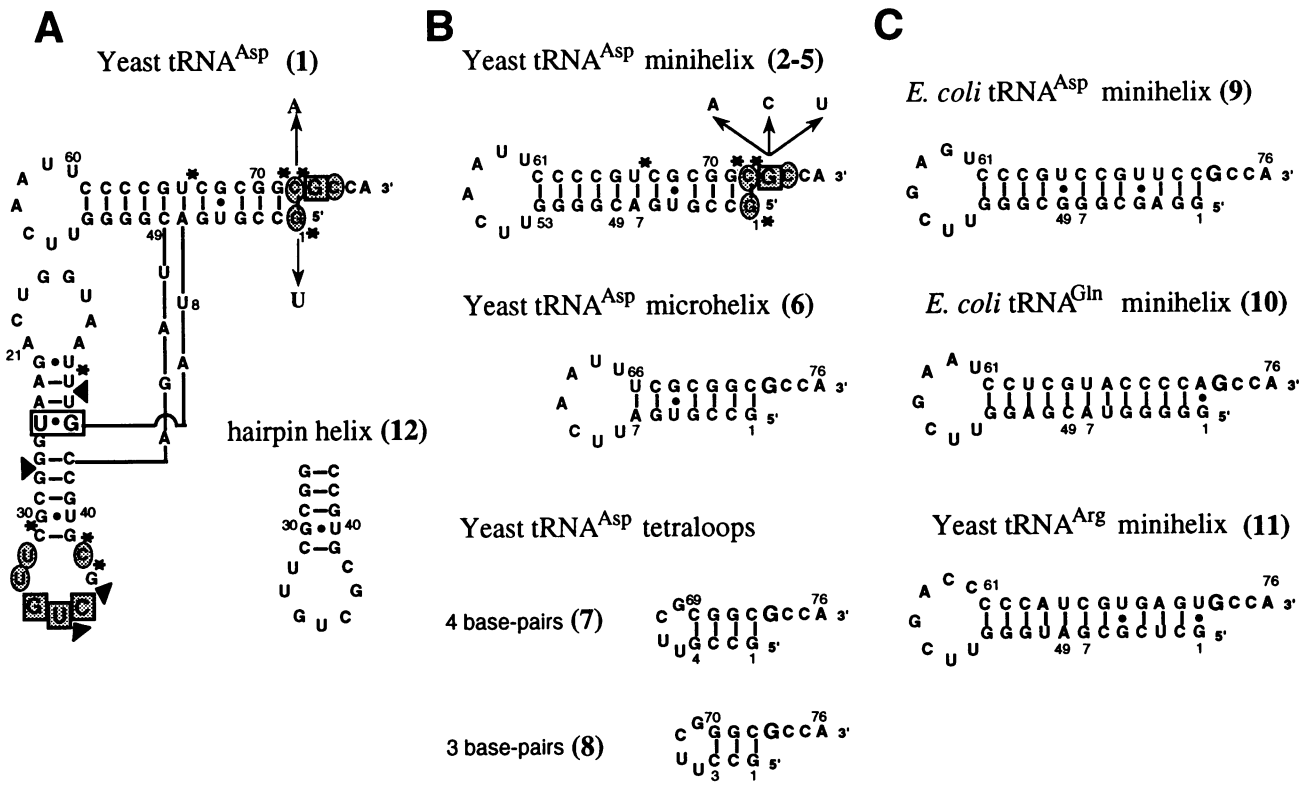

Fig. 1. Sequences of potential RNA substrates of yeast AspRS. (**A**) Yeast tRNA^{Asp} transcript (molecule 1) containing the G1–C72 base pair (for transcriptional reasons the U1–A72 wild-type pair was replaced by a G1–C72 pair). Identity nucleotides are boxed (Pütz *et al.*, 1991). Contacts with the synthetase as deduced from the crystal structure of the tRNA^{Asp}–AspRS complex (Cavarelli *et al.*, 1993) are highlighted: bases in direct contact with the synthetase are shaded (identity determinants are boxed, other residues are circled), triangles indicate contacts with ribose moieties and stars imply interactions with phosphates. Molecule 12 corresponds to the anticodon arm of tRNA^{Asp}. (**B**) Sequences of resected RNA helices recapitulating all or part of the tRNA^{Asp} acceptor branch (molecules 2–8). Identity nucleotide G73 is boxed in molecule 2 and its mutations in molecules 3–5 are indicated by arrows. Potential contacts of these mini-helices with AspRS are indicated as in (A). (**C**) Mini-helices derived from other tRNAs as indicated (molecules 9–11). Numbering of RNA sequences is by analogy to canonical tRNAs. Sequence data are from the compilation of Steinberg *et al.* (1993).

under optimal conditions reach 35% of the molecules. This value is very high as compared with aminoacylation of other tRNA-derived mini-helices bearing only one identity nucleotide, as for example the yeast mini-helix^{Val} which under the same conditions is charged only to ~2% (Figure 2A). The charging level of mini-helix^{Asp} is dependent on the synthetase concentration (Figure 2B) as well as on ionic strength (Figure 2C) and temperature (Figure 2D). Taking into account these effects, optimal aminoacylation conditions have been defined (20°C, no salt and a $MgCl_2$/ATP ratio of 15, see Materials and methods) and applied to further experiments.

Determination of Michaelis–Menten parameters under optimal aminoacylation conditions (Table I) shows that the catalytic efficiency (or kinetic specificity) of the mini-helix, defined as the ratio k_{cat}/K_m, is reduced 9000-fold as compared with that of yeast tRNA^{Asp} transcript. This effect is due to both higher K_m and decreased k_{cat} values.

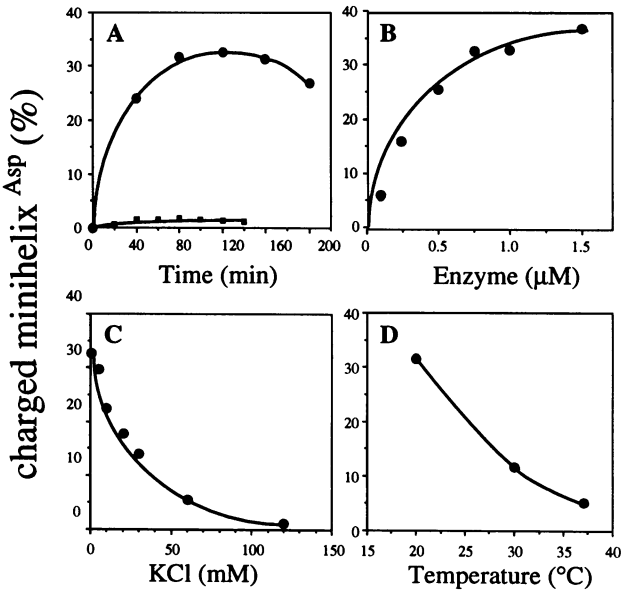

Fig. 2. Effect of experimental conditions on aspartylation of wild-type mini-helix^{Asp}. Effects on aminoacylation of incubation time (**A**), enzyme concentration (**B**), KCl concentration (**C**) and temperature (**D**). (A) The time course of mini-helix^{Asp} aminoacylation by yeast AspRS (circles) is compared with the valylation by yeast ValRS (squares) of a mini-helix derived from tRNA^{Val} (Frugier *et al.*, 1992). In all experiments, aspartylation assays were performed in the presence of 3 μM mini-helix and 0.75 μM AspRS [except in (B) where AspRS concentration varied from 0.1 to 1.5 μM]. Valylation assays were performed under the same experimental conditions in the presence of optimal concentrations of substrate (7 μM) and enzyme (0.84 μM). The temperature was 20°C in (A–C). No KCl was present in the experiments presented in (A, B and D).

Comparative aminoacylation of yeast tRNA^{Asp}-derived RNA mini-substrates

Three RNA hairpins derived from yeast mini-helix^{Asp} and varying in length and sequence of the loop (micro-helix, 4 bp tetraloop, 3 bp tetraloop) have been synthesized (Figure 1). They all contain the sole identity nucleotide present in the acceptor branch of tRNA^{Asp}, nucleotide G73. These hairpins have been tested for their aspartylation ability. As seen in Table I, all three RNAs remain substrates for yeast AspRS. Plateaus of aminoacylation still reach 25% with the micro-helix and 4–6% with the tetraloops. The kinetic parameters are also listed in Table I. Removal from mini-helix^{Asp} of the 5 bp corresponding to the T-stem has little effect on both K_m (2-fold increment) and k_{cat} (1.9-fold loss). Thus, aspartylation efficiency of micro-helix^{Asp} decreases by a factor 3.5 as compared with that of mini-helix^{Asp}.

Further shortening of the micro-helix by replacement of the 7 nt long T-loop by a tetraloop, and by reduction to 4 bp of the acceptor stem, has a weak global effect as compared with micro-helix^{Asp}. Indeed, the loss in efficiency of the 4 bp tetraloop is only ~9-fold as compared with mini-helix^{Asp}. This is in turn mainly due to a 15-fold increase in K_m. The K_m effect is amplified with the 3 bp tetraloop. Here K_m could not be measured precisely but was estimated to be >100 μM and thus ~30 times higher than the K_m of mini-helix^{Asp}. The rate constant k_{cat} remains about the same. Thus, the loss in aminoacylation efficiency of the 3 bp tetraloop is at least 45-fold.

Specificity of mini-helix aspartylation

To assess the specificity of aspartylation of mini-helix^{Asp}, three variants of this molecule, presenting alterations at the discriminator position, have been synthesized and submitted to aminoacylation assays. Replacing G73 by any of the three other possible nucleotides has a severe effect on the charging levels as well as on the aminoacylation efficiency (Table II). The effect of mutations varies with the nature of the nucleotide. Variants U73, A73 and C73 of the mini-helix correspond to losses in efficiency of 40-, 160- and 220-fold,

Table I. Kinetic parameters for aspartylation by yeast AspRS of resected RNA helices containing a G residue at discriminator position 73

Transcripts	Plateau (%)	k_{cat} (min^{-1})	K_m (μM)	$k_{cat}/K_{m\ (rel.)}$[a]	ℒ[b] relative to tRNA^{Asp} (*x*-fold)	ℒ[b] relative to mini-helix^{Asp} (*x*-fold)
Yeast tRNA^{Asp}	100.0	13.8	0.05	1.00	1	
Yeast mini-helix^{Asp}	35.0	0.11	3.5	1.14×10^{-4}	9000	1.0
Yeast micro-helix^{Asp}	25.0	0.057	6.6	3.13×10^{-4}	32 000	3.5
Yeast tetraloop^{Asp} (4 bp)	6.0	0.18	50.0	1.30×10^{-5}	77 000	8.7
Yeast tetraloop^{Asp} (3 bp)	4.0	0.07	>100	$<2.50 \times 10^{-6}$	>395 000	>45
E.coli mini-helix^{Asp}	40.0	0.04	1.8	8.05×10^{-5}	12 400	1.4
Yeast mini-helix^{Arg}	5.5	0.0031	1.8	6.20×10^{-6}	160 000	18.0
E.coli mini-helix^{Gln}	0.6	0.0026	1.6	5.90×10^{-6}	169 000	19.0

[a]Relative kinetic specificity constants are defined as $(k_{cat}/K_m)_{rel.} = (k_{cat}/K_m)_{mutant}/(k_{cat}/K_m)_{wild\text{-}type}$.
[b]ℒ-values are defined as inverses of $(k_{cat}/K_m)_{rel.}$ (for details see Pütz *et al.*, 1993). ℒ -values for duplicates varied by <20%.

Table II. Effect of mutation of the discriminator base 73 on aspartylation kinetics of yeast aspartate mini-helices and comparison with homologous tRNA transcripts

Transcripts	Plateau (%)	k_{cat} (min^{-1})	K_m (μM)	$k_{cat}/K_{m\ (rel.)}$[a]	$\mathcal{L}$ (x-fold)
Mini-helix^{Asp} G73 wt	35.0	0.11	3.50	1	1
tRNA^{Asp} G73 wt		*31.20*	*0.05*	*1*	*1*
Mini-helix^{Asp} U73	1.3	0.0026	3.50	0.023	40
tRNA^{Asp} U73		*0.058*	*0.20*	*0.028*	*36*
Mini-helix^{Asp} A73	0.9	0.0011	5.50	0.0063	160
tRNA^{Asp} A73		*0.019*	*0.29*	*0.0063*	*160*
Mini-helix^{Asp} C73	0.5	0.0014	9.70	0.0046	220
tRNA^{Asp} C73		*0.017*	*0.32*	*0.0051*	*200*

[a]See Table I legend.
$\mathcal{L}$ -values for duplicates varied by <20%. Data on aminoacylation kinetics of yeast full-length tRNA^{Asp} transcripts (displayed in italics) correspond to values from Pütz *et al.* (1991).

respectively. Michaelis–Menten constants are only weakly affected (at most a 3-fold increase). The main effect of the mutations is observed on the catalytic rate constant k_{cat} which is lowered ~40- to 100-fold. Interestingly, the effect of mutations increases in the following order: G > U > A > C. This is reminiscent of what was observed when mutating the discriminator position within the full-length tRNA^{Asp} transcripts (Pütz *et al.*, 1991) (Table II).

Aspartylation of non-cognate mini-helices

Three mini-helices derived from *E.coli* tRNA^{Asp} and tRNA^{Gln} and from yeast tRNA^{Arg} were also tested in aspartylation. These mini-helices share only the discriminator base G73 (in addition to the conserved nucleotides in tRNAs) with mini-helix^{Asp} and thus were expected to behave as efficient substrates for AspRS.

The *E.coli* aspartate mini-helix is a substrate for AspRS as efficiently as mini-helix^{Asp} (Table I). The level of charging is as high (35%), k_{cat} is reduced 3-fold and K_m is reduced 2-fold. Both yeast mini-helix^{Arg} and *E.coli* mini-helix^{Gln} are charged to low levels of aminoacylation with reduced k_{cat} values. Michaelis–Menten constants remain, however, the same as the K_m of *E.coli* mini-helix^{Asp} and very close to that of yeast mini-helix^{Asp}. The global loss in aspartylation efficiency for both mini-helices is ~20-fold as compared with yeast mini-helix^{Asp}.

Anticodon hairpin helix effects

When a hairpin helix mimicking the anticodon arm of yeast tRNA^{Asp} transcript (molecule 12 composed of 7 nt in the loop and 5 bp) is added to aminoacylation media already containing mini-helix^{Asp}, no stimulation of the charging level of this mini-helix could be detected (Table III). This contrasts with that found with a mini-helix derived from the acceptor arm of yeast tRNA^{Val} whose aminoacylation is specifically stimulated by the presence of an anticodon hairpin helix mimicking the anticodon arm of tRNA^{Val} (Frugier *et al.*, 1992). Instead, weak concentrations of the aspartate anticodon hairpin helix inhibit the charging of mini-helix^{Asp}, whereas mini-helix^{Val} aminoacylation is still stimulated at 25-fold higher concentrations of the anticodon helix (Table III). This indicates that the lack of aspartylation stimulation is not due to the absence of interaction of the hairpin helix with AspRS, and thus explicitly shows a different behavior of aspartate and valine hairpin helices during aminoacylation of the corresponding accepting mini-helices.

Table III. Effects of anticodon hairpin helices on the aminoacylation of RNA mini-helices in the aspartate and valine systems

Anticodon hairpin helix added	Mini-helix aminoacylation plateaus	
(μM)	aspartate system (%)	valine system[a] (%)
–	35	2.5
1.8	34	–
3.9	27	–
7	19	5.3
14	–	5.7
30	–	7.4
50	–	7.6

[a]Values from Frugier *et al.* (1992).
Concentration of accepting mini-helices was 3 μM in the aspartate and 7 μM in the valine system.

Discussion

Identity of yeast tRNA^{Asp} is governed by five determinants located symmetrically in three domains of the tRNA structure: (i) the accepting end for discriminator residue G73, (ii) the opposite extremity for the anticodon GUC triplet and (iii) the central hinge region of the L-shaped tRNA fold for base pair G10–U25 (Pütz *et al.*, 1991). As seen by crystallography, the determinants located at both extremities of the tRNA directly contact the two main structural domains of AspRS by hydrogen bonding, while the central G10–U25 pair is in close vicinity to the connecting region joining the catalytic core and the anticodon-recognizing module of the synthetase (Ruff *et al.*, 1991). Footprints of AspRS-complexed phosphorothioate-containing tRNA^{Asp} transcripts mutated at identity positions have shown that the specific contacts with the synthetase are lost at the mutated positions (Rudinger *et al.*, 1992b). Here we will interpret the aspartylation properties of minimalist RNA helices by AspRS in the light of the structural knowledge on the yeast aspartate system, before enlarging the discussion to mechanistic and evolutionary aspects of tRNA aminoacylation.

Mini-helix^{Asp} is an efficient and specific substrate for yeast AspRS

We demonstrate here that an aspartate mini-helix, possessing only one out of the five aspartate identity determinants, is an excellent substrate for yeast AspRS. As seen in Figure 2, up to 35% of the mini-helix molecules can be aspartylated. The incomplete charging is not a reflection of inactive molecules present in aminoacylation media, since in the presence of a variant AspRS >60% of the molecules are chargeable (unpublished result). In the presence of the yeast enzyme, optimal aspartylation of mini-helix^{Asp} is obtained after 60–80 min incubation. For longer incubations, the decrease of plateau levels (Figure 2A) is due to kinetic side effects (Bonnet and Ebel, 1972; Dietrich *et al.*, 1976) linked to the deacylation of mini-helices. Plateau levels are also decreased with an increase of ionic strength and temperature (Figure 2C and D). This probably reflects decreased affinities of the mini-helix for AspRS when the salt concentration increases, but also structural effects on the mini-helix itself which might be destabilized by increasing temperature.

Although aspartylation levels of mini-helix^{Asp} are high, the kinetic specificity for mini-helix aminoacylation is 9000-fold less efficient than that of wild-type tRNA^{Asp} (Table I). This is due firstly to the weaker affinity of mini-helix^{Asp} for AspRS. Indeed, the aspartylation K_m, which is a reflection of the inverse of affinity, increases from 0.05 μM for the whole tRNA to 3.5 μM for mini-helix^{Asp}. This may reflect a 70-fold affinity decrease for the mini-helix. Such a decrease is likely, because crystallography tells us that at least 20 hydrogen bonds between AspRS and complexed tRNA^{Asp} occur with residues from the anticodon branch (Cavarelli *et al.*, 1993), and thus are lost when this domain is removed. The less efficient aminoacylation of mini-helix^{Asp} is also linked to a decreased rate constant k_{cat}, that falls from 13.80 to 0.11 min^{-1}. This corresponds to a 125-fold decrease. In summary, the decrease in catalytic efficiency of mini-helix^{Asp} as compared with tRNA^{Asp} is equally a result of K_m (affinity) and k_{cat} effects.

Considering mini-helix^{Asp} as a tRNA^{Asp} mutant lacking anticodon and base pair G10-U25 identity elements, one can make a theoretical estimate of its catalytic efficiency for aspartylation in the case of single additivity of mutational effects. When compared with tRNA^{Asp}, the loss in kinetic specificity ($\mathcal{L}$) would be in the range of 4.0×10^5- to 2.5×10^8-fold [values derived from $\mathcal{L}_{mm} = \mathcal{R} \Pi \mathcal{L}_{sm}$, with $\mathcal{R} = 1$ (Pütz *et al.*, 1993) using either the lowest or highest $\mathcal{L}_{sm}$ values for the individual identity positions (Pütz *et al.*, 1991), with 'mm' for multiple mutants and 'sm' for single mutants]. These calculated values largely exceed the experimental value of 9000. Phenomenologically, this indicates that the mini-helix behaves as a strongly anti-cooperative tRNA^{Asp} mutant modified at anticodon and G10–U25 identity elements. We note that anti-cooperative effects were observed for a triple anticodon tRNA^{Asp} mutant (GUC replaced by CAU), only 3300-fold less efficient than the wild-type molecule (Pütz *et al.*, 1993). Following this view, our results imply that the anticodon domain of tRNA^{Asp} contributes only moderately to the catalytic efficiency of the synthetase. This implies further that determinant G73 would act essentially in an independent manner in the context of the whole tRNA and that the other identity elements would have a limited role in triggering the catalytic activation AspRS (see below).

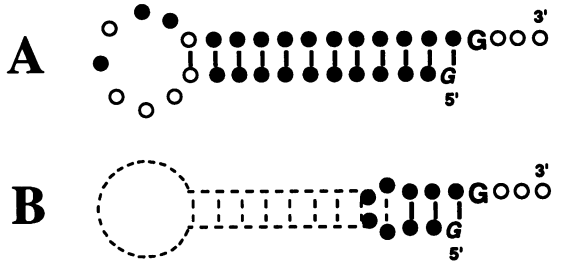

Fig. 3. (**A**) Consensus sequence of mini-helices aspartylated by yeast AspRS. Only two G residues are common between yeast aspartate, *E.coli* aspartate, *E.coli* glutamine and yeast arginine mini-helices. (●), non-conserved nucleotides among the four sequences studied; (○), nucleotides conserved in all tRNAs (Steinberg *et al.*, 1993). (**B**) Minimalist structural requirements of RNA helices to be charged by yeast AspRS. The RNA parts that can be removed are indicated by dashed lines.

To assay for specificity of mini-helix^{Asp} charging, mutants at identity position N73 were created. Replacement of identity determinant G73 by any of the three other nucleotides leads to a systematic loss in aspartylation activity. This loss varies from a factor of 40 to a factor of 220 and is essentially due to k_{cat} decreases. Interestingly, the ranking of N73 nucleotides according to their efficiency to activate AspRS (G > U > A > C) is the same as in the whole tRNA (Table II and Pütz *et al.*, 1991). Moreover, even though aminoacylation of mini-helices and tRNA was performed under slightly different conditions, the effects of mutations in both structural contexts are quantitatively similar for the moderate K_m and the more pronounced k_{cat} variations. This indicates that the discriminator position is recognized similarly within mini-helix^{Asp} and whole tRNA^{Asp}. Further, these data indicate that the major role of N73 residues is not to strengthen the binding of mini-helix^{Asp} to AspRS. Instead, they trigger activation of the catalytic center and contribute to the specificity of this event, because the greater the number of potential contacts of N73 with AspRS (G > U > A > C) (Cavarelli *et al.*, 1993; Pütz *et al.*, 1993) the better is the activation.

If discriminator base 73 is really the main element responsible for the catalytic activation of AspRS, other mini-helices containing a G73 residue, but with completely different sequences, should become chargeable by AspRS with the same kinetic specificity as mini-helix^{Asp}. Mini-helices derived from *E.coli* tRNA^{Asp} and tRNA^{Gln} and from yeast tRNA^{Arg} give these characteristics (Figure 1). In agreement with this view, these three mini-helices are charged by AspRS and their consensus sequence, displayed in Figure 3A, shows that only the G73 residue and the 5′-terminal G1 remain common, besides the conserved residues at the CCA$_{OH}$-end and T-loop. Mini-helix^{Asp} from *E.coli* behaves quasi-identically as yeast mini-helix^{Asp}, with similar kinetic constants (a moderate K_m effect compensated by an opposite k_{cat} effect). The two other mini-helices are only 20-fold less efficiently charged than yeast mini-helix^{Asp}. This indicates that the presence of G73 is sufficient to trigger catalysis by AspRS and that the other nucleotides within the mini-helix structure play a minor role.

The less efficient mini-helix^{Arg} and mini-helix^{Gln} charging

is mainly due to a k_{cat} effect. This could result from the presence of non-Watson–Crick base pairs at positions 1–72 in these RNAs (G1–U72 in mini-helix^{Arg} and G1–A72 in mini-helix^{Gln}, instead of a G1–C72 pair in aspartate mini-helices). Thus, contacts between the first base pair and AspRS are partly lost at nucleotide 72. Indeed, the N4 atom present at position C72 in both yeast and *E.coli* aspartate mini-helices has been replaced by an O4 atom at U72 in mini-helix^{Arg} and by an N1 atom at A72 in mini-helix^{Gln}. In mini-helix^{Gln} the N1 atom from A72 is presented to AspRS in a different orientation because of the geometry of the G–A base pair. The different kinetic parameters found for the heterologous arginine and glutamine mini-helices thus reflect the loss of one or more contacts between the discriminator base and the enzyme. This suggests that interactions other than those between the G73 base and the active site of the synthetase are needed to trigger aspartylation; these interactions involve chemical groups within base pairs 1–72 at the end of the acceptor branch of the tRNA. The presence of moderate antideterminants in the non-cognate mini-helices that may contribute additionally to their decreased activity is not excluded.

Minimalist structural features required for aspartylation

The X-ray structure of the aspartate complex shows that almost all interactions of the tRNA-accepting branch with AspRS concern residues near to the CCA_{OH}-end of the molecule (Cavarelli *et al.*, 1993). Because no interaction occurs with the T-arm and -loop, we tested the aminoacylation capacity of an aspartate micro-helix composed solely of the 7 bp of the amino-accepting arm of tRNA^{Asp} and closed by the aspartate T-loop (molecule 6 in Figure 1). This micro-helix contains all potential binding sites with AspRS and thus should be a good aspartate acceptor. As anticipated, micro-helix^{Asp} is aspartylated

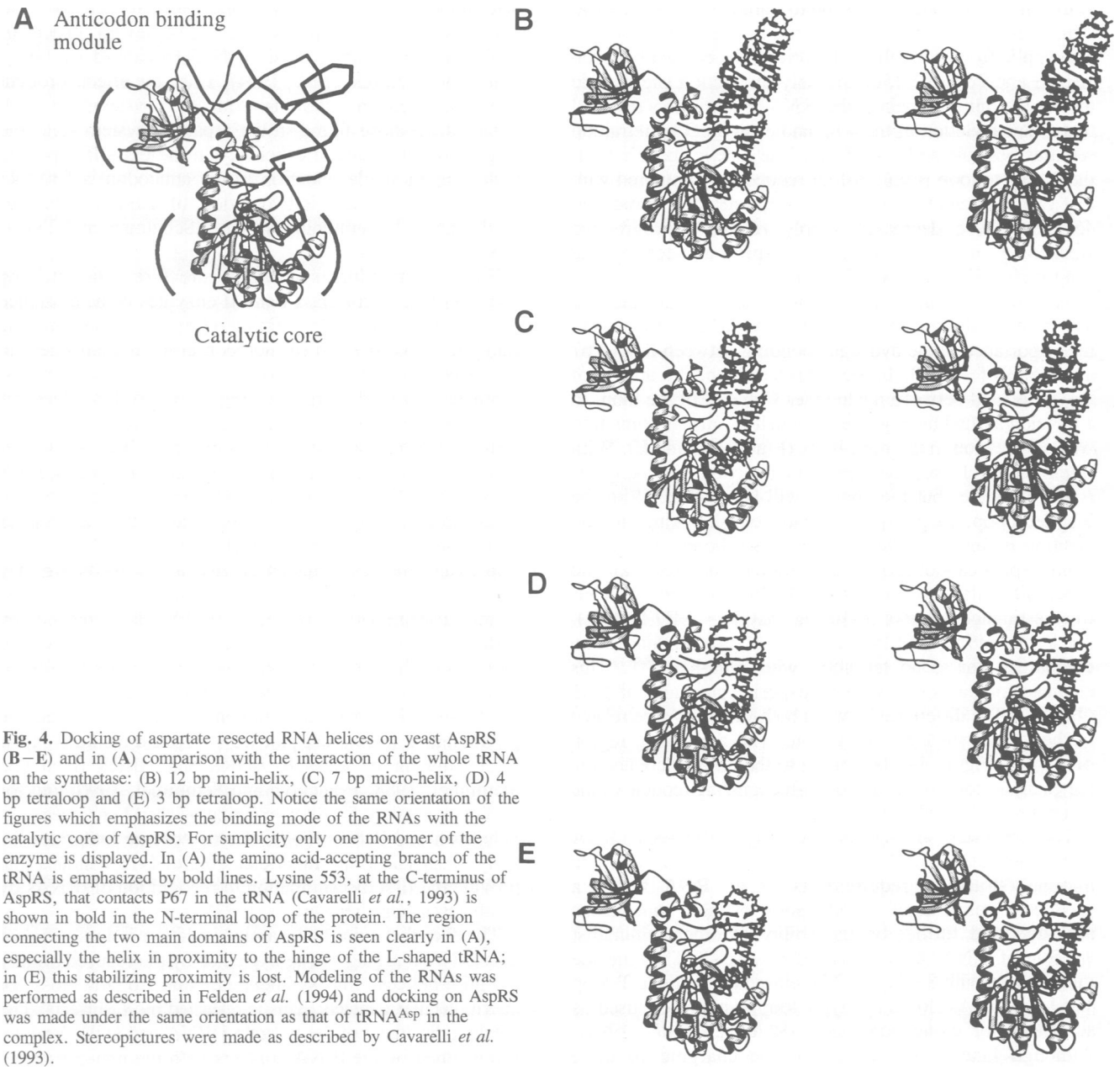

Fig. 4. Docking of aspartate resected RNA helices on yeast AspRS (**B**–**E**) and in (**A**) comparison with the interaction of the whole tRNA on the synthetase: (B) 12 bp mini-helix, (C) 7 bp micro-helix, (D) 4 bp tetraloop and (E) 3 bp tetraloop. Notice the same orientation of the figures which emphasizes the binding mode of the RNAs with the catalytic core of AspRS. For simplicity only one monomer of the enzyme is displayed. In (A) the amino acid-accepting branch of the tRNA is emphasized by bold lines. Lysine 553, at the C-terminus of AspRS, that contacts P67 in the tRNA (Cavarelli *et al.*, 1993) is shown in bold in the N-terminal loop of the protein. The region connecting the two main domains of AspRS is seen clearly in (A), especially the helix in proximity to the hinge of the L-shaped tRNA; in (E) this stabilizing proximity is lost. Modeling of the RNAs was performed as described in Felden *et al.* (1994) and docking on AspRS was made under the same orientation as that of tRNA^{Asp} in the complex. Stereopictures were made as described by Cavarelli *et al.* (1993).

almost as well as mini-helix^{Asp} (3.5-fold loss in catalytic efficiency). This confirms the non-importance of the T-arm in the aspartylation process and shows that the shifted orientation of the T-loop towards the synthetase by almost one half helical turn in the 7 and 12 bp long accepting helices does not introduce steric antideterminant effects. Docking mini-helix^{Asp} and micro-helix^{Asp} within the tRNA interaction site on AspRS explains this fact well. It is clearly seen that the T-arm protrudes out of the complex core and that the most compact structure is obtained by interaction of the micro-helix with AspRS (Figure 4B and C).

Because 14 out of the 15 interaction sites between the amino acid-accepting branch of tRNA^{Asp} and AspRS are clustered in base pairs 1–72 and the single-stranded G73CCA$_{OH}$-terminus, one could question whether shorter micro-helices would keep the potential to be aspartylated. To test this possibility, potential shorter RNA substrates were constructed. The 3 and 4 bp-containing RNAs were closed by stable tetraloops to prevent possible steric hindrance due to the bulky 7 nt long T-loop and to stabilize the short helical structures. Functional assays of the two tetraloops should also explicitly inform about the role of the contact between AspRS and P67, the 15th and only interaction site outside the very terminal domain of the tRNA. Experiments revealed that aminoacylation of the 4 bp and even the 3 bp tetraloop remains possible and significant. The kinetic specificity of the 4 bp tetraloop is only 9-fold reduced as compared with that of mini-helix^{Asp}; that of the 3 bp tetraloop is reduced 45-fold. These decreases simply reflect a progressive weakening of their affinity for AspRS as seen by the progressive K_m increase (Table I).

Modelling of mini-helix^{Asp}, micro-helix^{Asp} and the two aspartate tetraloops, and docking on AspRS, clearly shows the importance of the hydrogen bonding between RNA P67 and K553 of AspRS. In the 4 bp tetraloop, the analog of P67 is located between nucleotides C and G of the loop, in a position shifted by a quarter of a helical turn as compared with its location in the mini-helix (Figure 4D and E). With slight structural rearrangements an interaction with the lysine is still possible, but the contact will be weaker. With the 3 bp tetraloop, the phosphate capable of mimicking the P67 position is further shifted and hydrogen bonds with K553 from AspRS cannot form. Calculation of the loss in kinetic specificity, after the loss of this hydrogen bonding, leads to an estimated value of 30 [using $\Delta\Delta G\dagger = -RT\ln(1/\mathcal{L})$, see Fersht (1985) and Pütz *et al.* (1993) for details] when comparing the 3 bp tetraloop with mini-helix^{Asp}. This estimate compares well with the experimental value of >45 (Table I). The difference between both values may be related to the loss of stacking interactions with the helical region of AspRS (Figure 4A) belonging to the domain connecting the catalytic core to the anticodon-recognizing module of the synthetase (Cavarelli *et al.*, 1993).

The conclusions arising from the study of 10 resected RNA helices are summarized in Figure 3B which schematizes the minimal structural requirements of an RNA to be a productive substrate of AspRS. Some of these conclusions are supported further by the ability of other minimalist versions of tRNA^{Asp} to be charged by AspRS. They include mini-helices with 8–11 or 13 bp closed by a classic T-loop and 12 bp RNAs closed by atypic loops which were used as substrates for elongation factor (Rudinger *et al.*, 1994). Although kinetic parameters for the charging of these molecules remain to be measured, their significant chargeability confirms that aspartylation is insensitive to the sequence, structure and orientation of the T-loop, as well as to the length of the accepting helix.

Mini-helix charging by class I and II synthetases: mechanistic and evolutionary aspects

The efficient charging of mini-helix^{Asp} shows that yeast AspRS behaves like other class II synthetases that aminoacylate mini-helices. However, in contrast to AlaRS and SerRS that do not present specificity determinants in the anticodon, or to HisRS and GlyRS where anticodon plays a minor role in identity, yeast AspRS recognizes all three anticodon nucleotides of its cognate tRNA as strong determinants, equally well as the N73 discriminator determinant. In this respect, AspRS deviates from class I synthetases charging mini-helices (IleRS, MetRS, ValRS) that need both discriminator and anticodon nucleotides as identity determinants. For those synthetases, anticodon determinants have extremely strong effects on activity, with kinetic specificity constants that can be several orders of magnitude larger than those at N73 (reviewed by Giegé *et al.*, 1993; Nureki *et al.*, 1994). Thus, the effects brought about by anticodon determinants in class I systems are much greater than those found in the aspartate system [e.g. the largest loss in catalytic efficiency in the class II aspartate system upon single mutation in the anticodon is 530-fold (Pütz *et al.*, 1991); it is two orders of magnitude greater in the class I methionine system (Schulman and Pelka, 1988)].

When comparing synthetase structure, the striking common feature for class I and II enzymes is the existence of (i) conserved class-defining domains containing the catalytic active site and (ii) non-conserved domains needed for contacts with distal parts of the tRNA, including for most synthetases a module recognizing the anticodon (Buechter and Schimmel, 1993; Moras, 1993; Schimmel *et al.*, 1993). This implies that early synthetases may have been active site-containing minimalist proteins recognizing minimalist RNA substrates. With these considerations, the primary determinant specifying tRNA aspartylation by yeast AspRS is residue N73. It triggers activation of the catalytic site of AspRS and ensures partial specificity, a conclusion that may be extended to other synthetases. Higher specificity and better discrimination between tRNAs is achieved by additional identity elements contacting the non-conserved modules of the synthetases but also possibly the conserved cores. In contemporary aminoacylation systems, the effects of these additional determinants may have become predominant, as for base pair G3–U70 and residue –1 for discrimination by class II AlaRS and HisRS (Hou and Schimmel, 1988; Francklyn and Schimmel, 1990) and for anticodon residues for discrimination by class I enzymes (e.g. Schulman and Pelka, 1988). Such a scheme integrates the early proposal on the functional role of N73 residues that provide the first discrimination in recognition of tRNAs by synthetases (Crothers *et al.*, 1972).

The fact that mini-helix aminoacylation is less efficient than tRNA charging can be explained by the reduced affinity of mini-helices for synthetases, due to the loss of intermolecular contacts. This is reflected by K_m effects. The precise adjustment of the accepting tRNA-end in the catalytic site is tuned by the tRNA contacts with the non-conserved

modules of synthetases. In the present case these contacts occur between the aspartate anticodon and the β-barrel module of AspRS (Figure 4A). Optimal contacts, that 'freeze' the functional conformation of the synthetase, lead to optimal k_{cat} values. Those contacts are possible if distal interaction sites on the synthetase are activated by the primary interaction between the accepting-end of the tRNA and active site domain of the protein. This requires a mutual adaptation of tRNA and synthetase with a synthetase-induced conformational change of the tRNA, which is revealed by the X-ray structure of the tRNA−synthetase complex (Ruff *et al.*, 1991). This tRNA conformation is constrained. If so, mutations of identity positions in the distal part of the tRNA would lead to moderate decreases in affinity due to losses of specific contacts. As a result, the constrained tRNA conformation becomes slightly relaxed. Hence, slight changes in the mutual adaptation of tRNA and AspRS occur. This is reflected by decreased k_{cat} values. In the case of double mutants, these effects are probably amplified and in the case of delocalized mutations at identity positions, relaxation of constraints (or creation of novel constraints due to alternative interactions) can explain the cooperative effects observed with $tRNA^{Asp}$ (Pütz *et al.*, 1993). The conformational changes, which might reflect such phenomena, have been revealed in footprinting experiments with variant tRNAs (Rudinger *et al.*, 1992b).

For certain multiple mutants, like $tRNA^{Asp}$ triple anticodon mutant (GUC→CAU) (Pütz *et al.*, 1993), relaxation of the tRNA may become too severe, so that all specific contacts with AspRS at anticodon positions are no longer possible. Thus, conformation of complexed tRNA becomes completely unconstrained and mutants behave like a minihelix. Noticeable and in agreement with this view, the anticooperative CAU $tRNA^{Asp}$ anticodon mutant has similar kinetic properties to mini-$helix^{Asp}$ (3300- and 9000-fold loss in kinetic specificity, respectively).

Comparing ΔG at the transition state of the aminoacylation reaction of $tRNA^{Asp}$ and resected RNA substrates permits the estimation of the energetic cost of the structural constraints within complexed tRNA or, in other words, that of the conformational change of $tRNA^{Asp}$ in the complex with AspRS. This cost is high and represents at least 7 kcal/mol (if only additive mutational effects are taken into account), but could reach 25 kcal/mol (if the loss of hydrogen bond contacts between the anticodon region of tRNA and AspRS is considered). A significant part of this energy corresponds to the conformational rearrangement of the anticodon loop that unstacks identity bases for optimal presentation to AspRS. Another contribution probably originates from the bending of the L-shaped tRNA which leads to the D-loop rearrangement at the hinge of the two tRNA branches (Ruff *et al.*, 1991; Cavarelli *et al.*, 1993). An energetic contribution for conformational changes within the enzyme is not excluded.

In summary, these structural arguments support the view of an independent functioning of the catalytic domain of AspRS, in agreement with the phenomenological arguments discussed above. This conclusion may be extended to other class II synthetases that would have retained the ability to recognize in their contemporary substrates identity signals from an early code that specified aminoacylation of proto-tRNAs. The primordial role of discriminator residue N73 would then rationalize the surprising chargeability by class II LysRS of a poly(U) oligonucleotide terminated by a CCA_{OH}-end (Khvorova *et al.*, 1992), in which the most 3′-U of poly(U) mimics discriminator residues of $tRNA^{Lys}$. In this minimalist single-stranded RNA, the distal 5′-domain of poly(U), mimicking the UUU anticodon of $tRNA^{Lys}$, would specifically anchor the RNA on the synthetase. Because class II synthetases recognize specifically and charge efficiently simplified substrates, they appear more primitive than class I synthetases that charge such substrates less efficiently. The experiments on the effects of hairpin helices on the chargeability of accepting helices support this view. Indeed, because aspartate anticodon hairpin helix does not stimulate charging of mini-$helix^{Asp}$ suggests that communication between AspRS domains is less elaborate than in class I synthetases, where stimulatory effects occur (Frugier *et al.*, 1992; Nureki *et al.*, 1993). In conclusion, these experiments on minimalist RNA substrates of yeast AspRS allowed us to determine the subtle mechanistic interplay between the identity elements of a tRNA. This would not have been possible by simple mutational analysis on the whole tRNA.

Materials and methods

RNA and enzymes

Oligodeoxynucleotides were synthesized on an Applied Biosystems 381A DNA synthesizer using the phosphoramidite method and purified by HPLC on a nucleosyl 120-5-C18 column (Bischoff Chromatography, Zymark-France, Paris, France). Concentrations of RNA transcripts were determined spectrophotometrically using extinction coefficients at 260 nm of 70.4×10^4 $M^{-1}cm^{-1}$ for wild-type $tRNA^{Asp}$ (molecule 1), 31×10^4 $M^{-1}cm^{-1}$ for mini-helices (molecules 2−5 and 9−11), 20.7×10^4 $M^{-1}cm^{-1}$ for micro-$helix^{Asp}$ (molecule 6), 13.6×10^4 $M^{-1}cm^{-1}$ for hairpin helix (molecule 12) and 10.2×10^4 $M^{-1}cm^{-1}$ for tetraloop substrates (molecules 7 and 8). These values were calculated according to Puglisi and Tinoco (1989). Ribonucleotides were obtained from Sigma (St Louis, MO). L-[^{3}H]aspartic acid (23 Ci/mol) was purchased from Amersham France (Les Ulis, France). T7 RNA polymerase (Wyatt *et al.*, 1991) and pure yeast AspRS (Lorber *et al.*, 1983) were purified as described previously.

Preparation of mini-helices

In vitro transcriptions were performed for 4 h at 37°C in mixtures containing 40 mM Tris−HCl (pH 8.1), 5 mM dithiothreitol, 5 mM spermidine, bovine serum albumin at 50 μg/ml, 40 mM $MgCl_2$, 4 mM of each nucleoside triphosphate, 5 mM GMP, 1 μM of each DNA strand (17mer for the plus strand and up to 52mer for minus strands), and 3000 U T7 RNA polymerase. Before transcription both DNA strands were hybridized by heating for 3 min at 60°C and slow cooling. Full-length transcripts were purified on 15 or 20% preparative denaturing polyacrylamide−8 M urea gels. This step allowed the separation of the CCA_{OH}-terminating transcripts from contaminating inactive molecules (abortive products and $n + 1$ or $n + 2$ transcripts). Control full-length $tRNA^{Asp}$ (molecule 1) was produced as described previously (Perret *et al.*, 1989). Molecules 2−5 and 7−12 were transcribed from single-stranded synthetic templates (Francklyn and Schimmel, 1989; Milligan and Uhlenbeck, 1989) and molecule 6 in the conventional way using double-stranded templates. Transcriptions were usually performed in 1 ml reaction mixtures, yielding between 5000 and 10 000 pmol purified RNA for molecules 2−5, 7 and 9−12. For molecule 6, the yield was about two times better, due to the double-stranded template used (18 000 pmol/ml transcription mixture). Molecule 8 was badly transcribed because of the shortness of the template (<1500 pmol/ml transcription mixture).

Aminoacylation reactions

All aminoacylation reactions were performed in the same medium containing 25 mM Tris−HCl (pH 7.5), 7.5 mM $MgCl_2$, 0.5 mM ATP, 0.1 mg/ml bovine serum albumin and 50 μM ^{3}H-labeled aspartic acid. Plateau experiments were performed with aspartate mini-helices at 3 μM and between 0.1 and 1.5 μM AspRS. Kinetic parameters were determined in the presence of 0.25 or 0.5 μM AspRS and transcript concentrations from 2.5 to 10 μM. Transcripts were renatured before aminoacylation by heating to 65°C for

90 s and slow cooling to room temperature. Incubations were at 20°C and aminoacylated tRNA samples were quenched and treated in the conventional way (Perret *et al.*, 1990), except that DE81 Whatmann paper was used instead of 3MM paper. This allowed a better recovery of precipitated mini-substrates (Frugier *et al.*, 1992). The kinetic parameters were derived from Lineveaver–Burk plots. They represent the averages of at least two independent experiments.

Acknowledgements

We thank P.Schimmel (MIT), S.Yokoyama (Tokyo) and D.Moras (Strasbourg), our partners in the HFSP project, for discussions on minimalist RNA structures and their relation with evolution of the genetic code. We thank G.Eriani, J.Gangloff, D.Kern and A.Théobald-Dietrich for discussions and synthetase samples and J.Rudinger, M.Sprinzl and their colleagues for unpublished data on mini-helices. Particular thanks are due to B.Felden for fruitful suggestions and modeling minimalist RNA structures, to J.Cavarelli for discussions and help in preparing Figure 4 and to A.Hoeft for synthesizing the oligonucleotides. This work was supported by grants from the Centre National de la Recherche Scientifique (CNRS), Ministère de la Recherche et de l'Enseignement Supérieur (MRES), Université Louis Pasteur, Strasbourg and the Human Frontier Science Program. M.F. was supported by a fellowship from MRT.

References

Bonnet,J. and Ebel,J.-P. (1972) *Eur. J. Biochem.*, **31**, 335–344.
Buechter,D.D. and Schimmel,P. (1993) *C. R. Biochem. Mol. Biol.*, **28**, 309–322.
Cavarelli,J., Rees,B., Ruff,M., Thierry,J.-C. and Moras,D. (1993) *Nature*, **362**, 181–184.
Cheong,C., Varani,G. and Tinoco,I.,Jr (1990) *Nature*, **346**, 680–682.
Crothers,D.M., Seno,T. and Söll,D.G. (1972) *Proc. Natl Acad. Sci. USA*, **69**, 3063–3067.
Cusack,S., Berthet-Colominas,C., Härtlein,M., Nassar,N. and Leberman,R. (1990) *Nature*, **347**, 249–255.
Dietrich,A., Kern,D., Bonnet,J., Giegé,R. and Ebel,J.-P. (1976) *Eur. J. Biochem.*, **70**, 147–158.
Ebel,J.-P., Giegé,R., Bonnet,J., Kern,D., Befort,N., Bollack,C., Fasiolo,F., Gangloff,J. and Dirheimer,G. (1973) *Biochimie*, **55**, 547–557.
Eriani,G., Delarue,M., Poch,O., Gangloff,J. and Moras,D. (1990) *Nature*, **347**, 203–206.
Felden,B., Florentz,C., Giegé,R. and Westhof,E. (1994) *J. Mol. Biol.*, **235**, 508–531.
Fersht,A. (1985) *Enzyme, Structure and Mechanism.* Freeman, NY.
Florentz,C. and Giegé,R. (1994) In Söll,D. and RajBhandary,U.L. (eds), *Transfer RNA*. American Society for Micro-biology, Washington, DC, in press.
Francklyn,C. and Schimmel,P. (1989) *Nature*, **337**, 478–481.
Francklyn,C. and Schimmel,P. (1990) *Proc. Natl Acad. Sci. USA*, **87**, 8655–8659.
Francklyn,C., Shi,J.-P. and Schimmel,P. (1992) *Science*, **255**, 1121–1125.
Frugier,M., Florentz,C. and Giegé,R. (1992) *Proc. Natl Acad. Sci. USA*, **89**, 3990–3994.
Giegé,R., Puglisi,J.D. and Florentz,C. (1993) *Progr. Nucleic Acid Res. Mol. Biol.*, **45**, 129–206.
Hou,Y.M. and Schimmel,P. (1988) *Nature*, **333**, 140–145.
Khvorova,A.M., Motorin,Y.A., Wolfson,A.D. and Gladilin,K.L. (1992) *FEBS Lett.*, **314**, 256–258.
Lorber,B., Kern,D., Dietrich,A., Gangloff,J., Ebel,J.-P. and Giegé,R. (1983) *Biochem. Biophys. Res. Commun.*, **117**, 259–267.
Martinis,S.A. and Schimmel,P. (1992a) *Proc. Natl Acad. Sci. USA*, **89**, 65–69.
Martinis,S.A. and Schimmel,P. (1992b) *J. Biol. Chem.*, **268**, 6069–6072.
Meinnel,T., Mechulam,Y., Blanquet,S. and Fayat,G. (1991) *J. Mol. Biol.*, **220**, 205–208.
Milligan,J.F. and Uhlenbeck,O.C. (1989) *Biochemistry*, **28**, 2849–2855.
Moras,D. (1993) *Biochimie*, **75**, 651–657.
Musier-Forsyth,K. and Schimmel,P. (1992) *Nature*, **357**, 513–515.
Musier-Forsyth,K. and Schimmel,P. (1993) *FASEB J.*, **7**, 282–289.
Nureki,O. *et al.* (1993) In Nierhaus,K. (ed.), *The Translation Apparatus*. Plenum Press, New York, 59–66.
Nureki,O., Niimi,T., Muramatsu,T., Kanno,H., Kohno,T., Florentz,C., Giegé,R. and Yokoyama,S. (1994) *J. Mol. Biol.*, **236**, 710–724.
Perret,V., Florentz,C., Dreher,T. and Giegé,R. (1989) *Eur. J. Biochem.*, **185**, 331–339.
Perret,V., Garcia,A., Grosjean,H., Ebel,J.-P., Florentz,C. and Giegé,R. (1990) *Nature*, **344**, 787–789.
Puglisi,J.D. and Tinoco,I.,Jr (1989) *Methods Enzymol.*, **180**, 304–325.
Pütz,J., Puglisi,J.D., Florentz,C. and Giegé,R. (1991) *Science*, **252**, 1696–1699.
Pütz,J., Puglisi,J.D., Florentz,C. and Giegé,R. (1993) *EMBO J.*, **12**, 2949–2957.
Rudinger,J., Florentz,C., Dreher,T. and Giegé,R. (1992a) *Nucleic Acids Res.*, **20**, 1865–1870.
Rudinger,J., Puglisi,J.D., Pütz,J., Schatz,D., Eckstein,F., Florentz,C. and Giegé,R. (1992b) *Proc. Natl Acad. Sci. USA*, **89**, 5882–5886.
Rudinger,J., Blechschmidt,B., Ribeiro,S. and Sprinzl,M. (1994) *Biochemistry*, in press.
Ruff,M. *et al.*, *Science*, **252**, 1682–1689.
Sampson,J.R. and Saks,M.E. (1993) *Nucleic Acids Res.*, **21**, 4467–4475.
Schimmel,P., Giegé,R., Moras,D. and Yokoyama,S. (1993) *Proc. Natl Acad. Sci. USA*, **90**, 8763–8768.
Schulman,L.H. and Pelka,H. (1988) *Science*, **242**, 765–768.
Steinberg,S., Misch,A. and Sprinzl,M. (1993) *Nucleic Acids Res.*, **21**, 3011–3015.
Wyatt,J.R., Chastain,M. and Puglisi,J.D. (1991) *BioTechniques*, **11**, 764–769.

Received on December 20, 1993